Radiofrequency emission by runaway electrons in FTU

P. Buratti[1], W. Bin[2], A. Cardinali[1], D. Carnevale[3], C. Castaldo[1], O. D'Arcangelo[1], F. Napoli[1], G.L. Ravera[1], A. Selce[1], L. Panaccione[1] and FTU Team[4]

[1]ENEA, Fusion and Nuclear Safety Department, C.R. Frascati, Via E. Fermi 45, 00044 Frascati (Roma) Italy. [2]ISTP-CNR, via R. Cozzi 53, 20125 Milano, Italy. [3]Dip. di Ing. Civile ed Informatica, Università di Roma Tor Vergata, Italy. [4]See the author list of G. Pucella et al., Nucl. Fusion 59, 112015 (2019).

1. Motivation

- Collective interactions with plasma waves can enhance RE pitch-angle scattering, leading to larger synchrotron losses, which in turn:
  - raise the critical electric field for avalanche multiplication
  - and reduce the maximum energy of RE.
- Emission of radio waves by runaway electrons has been studied on FTU tokamak under different plasma regimes, including:
  - low-density hot plasmas,
  - pellet-fueled plasmas,
  - post-disruption RE beams.

Buratti et al 2021 PPCF
https://doi.org/10.1088/1361-6587/ac138c

- The interest of post-disruption RE beams is obvious.
- Scenarios with hot, low-density background plasma are of interest for ITER startup.

2. Wave diagnostics

- Radio waves generated by coupling with plasma waves were collected by a wideband (log-periodic) antenna placed outside the vacuum vessel, in front of the exit of a vertical port closed by a dielectric window.

- The cutoff frequency due to propagation in the port was about 400 MHz.
- The antenna signal was acquired by a NI PXIe-5186 fast digitizer, with 5 GHz analog bandwidth and 8-bit resolution.

3. Wave detection in hot low-density plasmas

Figure 1

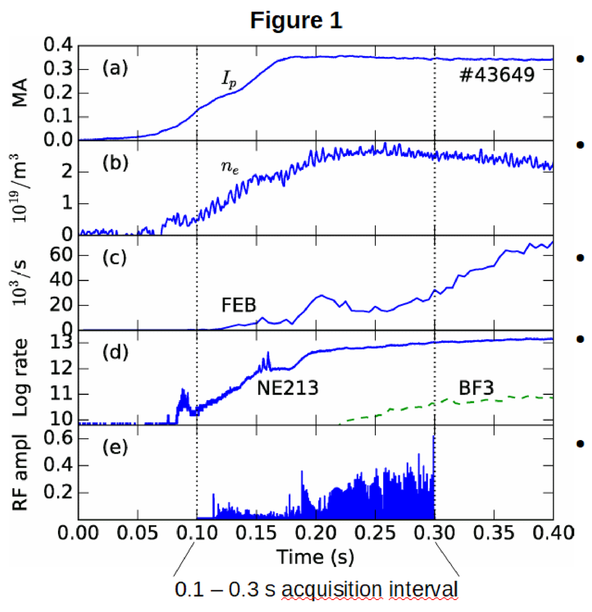

- Plasma current
- Line average density
- Hard-x from in-flight RE
- Hard-x + neutrons (NE213) & neutron contribution (BF3)
- Radio emission amplitude, normalized to digitizer saturation.

4. Wave detection in hot low-density plasmas (Fig. 1)

- Radiofrequency emissions have been detected in all examined discharges in which significant RE signatures, in particular HXR emission, were present.
- The background plasma temperature increases from 1.1 to 2.9 keV during the fast digitizer acquisition interval shown in Fig. 1.
- The amplitude of radio emission is estimated by moving RMS on 1 microsecond intervals.
- **Radio emission is intermittent.**
- Intermittency is common to all examined pulses.
- There is no correlation between radio bursts timing and MHD activities.
- The first radio burst appears during current ramp-up (t = 0.114 s), showing that kinetic instabilities influence RE dynamics already in the formation phase.

5. Shapes of radiofrequency bursts

Figure 2

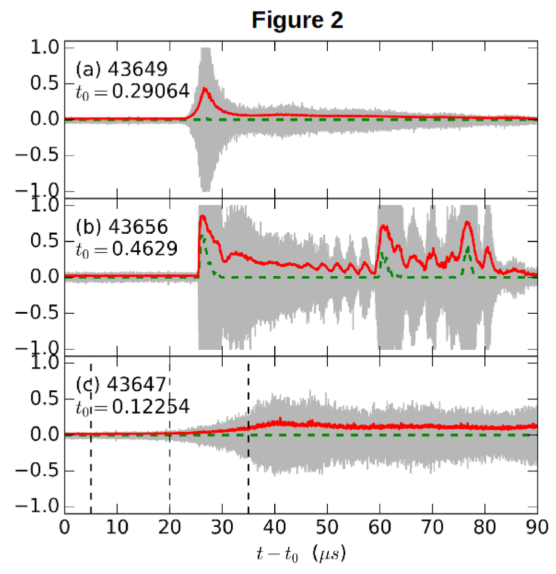

- A case with intermediate RE population (pulse shown in Fig. 1).
- A case with extreme RE population
- A case with weak RE population

6. Shapes of radiofrequency bursts (Fig. 2)

- RF signals normalized to digitizer saturation amplitude are shown by traces in grey.
- The amplitude estimated by moving RMS on 100 ns intervals is shown in red.
- The fraction of raw datapoints which saturate the digitizer dynamic range is shown in dashed green.
- The radio burst in the top frame grows exponentially for 5 microseconds, with a growth rate of about 10^6 /s;
- the quiescent period elapsed from the previous burst is 1.27 ms, which exceeds the growth rate by three orders of magnitude.
- The case with high RE content has very sharp leading edge and complex tail structure, with ringing oscillations and a second sharp rising front.
- The case with low RE content (bottom frame) has low amplitude and much smaller (10^5 /s) growth rate.

7. Correlation with ECE and RE losses

Figure 3

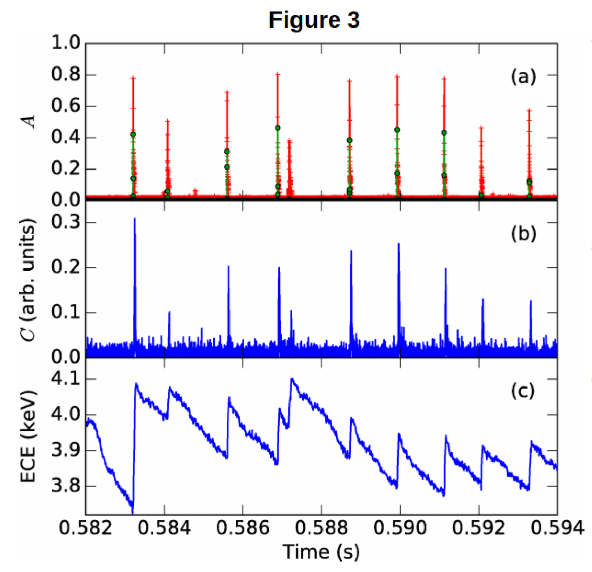

- Normalized RF amplitude from RMS (red) and fraction of saturated datapoints (green).
- Cherenkov probe signal
- Suprathermal ECE radiation temperature at 370 GHz.

8. Correlation with ECE and RE losses (Fig. 3)

- Rapid variations of the electron distribution function are spotted out from suprathermal ECE and Cherenkov probe fast channels.
- Radio bursts are accompanied in most cases by upwards steps of ECE and by bursts of the Cherenkov signal, as exemplified in figure 3.
- Both observations indicate enhanced pitch angle scattering, in fact rapidly increasing suprathermal ECE (on time scales shorter than RE acceleration time) is a sign of increasing RE perpendicular momentum, while bursts of the Cherenkov signal reveal temporarily enhanced RE losses.
- Only a small fraction of the RE population is ejected at each event, in fact the ECE signal remains strongly suprathermal all the time.

9. Spectral broadening

Figure 4

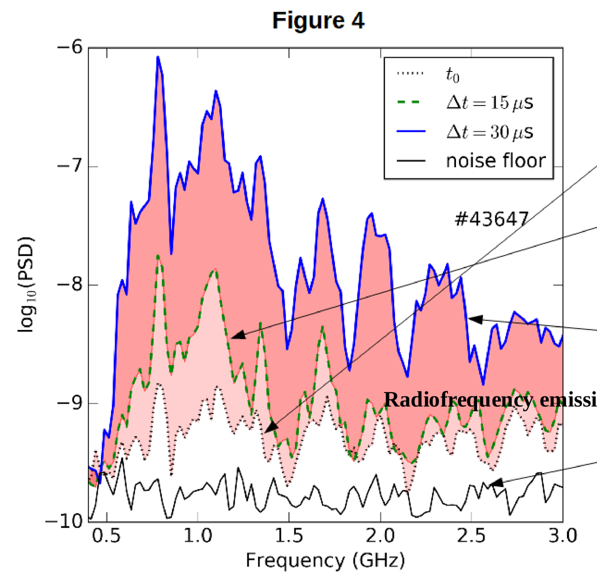

Power spectral densities:

- Just before a radio burst (dotted)
- During early exponential growth (dashed)
- At 60% of maximum amplitude (solid)
- Noise floor in the absence of RE

10. Spectral broadening (Fig. 4)

- Welch's power spectral densities (on 20 intervals of 256 points), from pulse 43647 at B = 4 T, at times shown by vertical dashed lines in Fig. 2c.
- The dotted line is a spectrum taken just before a radio burst (representative of low emission between bursts).
- The dashed line shows a PSD during the early growth phase, when amplitude is 13% of the maximum one: Significant changes occur in a relatively narrow range, from 0.6 to 1.7 GHz, as emphasized by the lighter shading in Fig. 4.
- The blue solid line shows the PSD at a time when amplitude is 60% of the maximum one: **There is substantial broadening with respect to the early growth phase**, as highlighted by the darker shading.
- Spectral broadening occurring on a time scale comparable to the amplitude e-folding time is indicative of strongly nonlinear wave coupling, a possible mechanism for rapid growth after relatively long stationary periods.

11. Coherent emissions

Figure 5

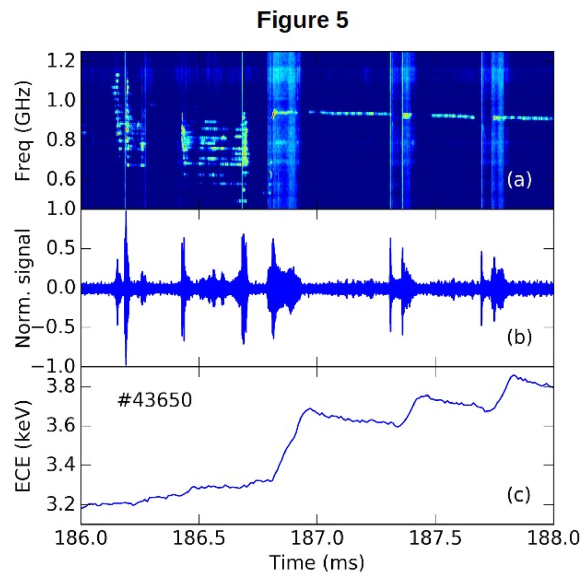

- Spectrogram of radiofrequency emission
- Raw signal normalized to saturation voltage
- ECE radiation temperature at 370 GHz

12. Coherent emissions (Fig. 5)

- There is multiline excitation at first,
- followed by broadband emission periods alternating with single-line spectra.
- the ECE signal slope only increases during periods of broadband emission.

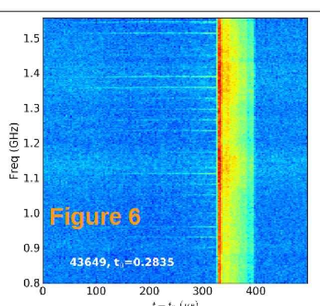

- Another instance of multiline excitation.
- Coherent lines appear in some cases before a radio burst.
- Line spacing is 31 MHz = ion cyclotron frequency at the low field side plasma periphery.

- Coherent emissions are also present during current ramp-up.
- Substantial work on their interpretation is in progress.

13. Pellet injection

Figure 7

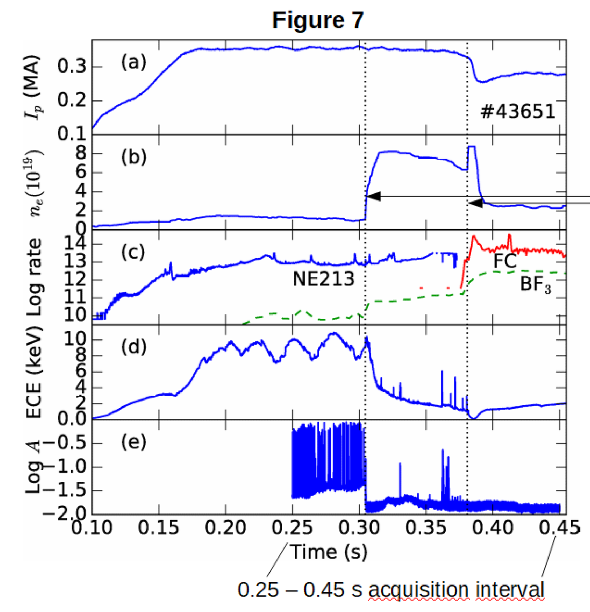

- Plasma current
- Line average density
- Pellets
- Hard-x + neutrons (NE213) & neutron contribution (BF3 & fission chambers)
- ECE
- Radio emission log amplitude, normalized to digitizer saturation.

14. Pellet injection (Fig. 7)

- Pellet injection on a target with large RE content.
- Intense radiofrequency bursts superposed to a continuous emission level are present before pellet injection, panel (e).
- The first pellet (t=0.304) produces a dense (8.3 10^19 /m^3), warm (0.5 keV) background plasma
- A substantial RE population survives pellet injection, indeed total HXR emission remains high, panel (c).
- Radio bursts disappear after pellet injection.
- The baseline emission decreases by a fator 5 within 0.9 ms after pellet injection.
- The second pellet provokes a disruption; the background plasma becomes very cold.
- Radio emission temporarily disappears during this phase, but see figure 8 below.

15. Post-disruption RE beam

Figure 8

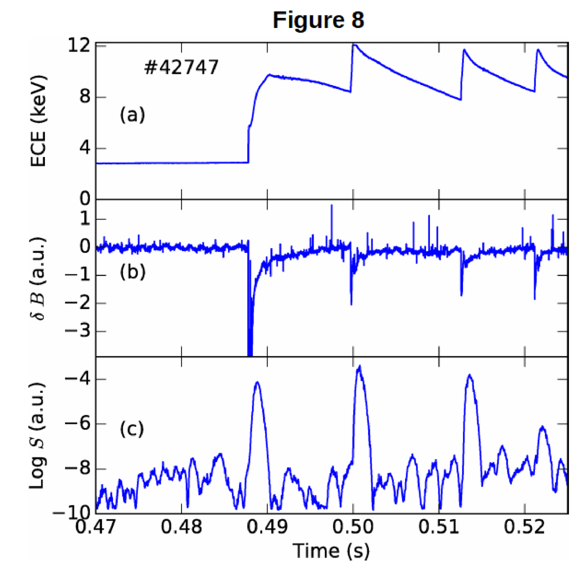

- ECE radiation temperature at 370 GHz
- Mirnov coil signal, showing macroscopic prturbations; the first spike is out of scale.
- Radio emission at 500 MHz, as measured by an analog spectrum analyzer.

16. Post-disruption RE beam (Fig. 8)

- Radio emission temporarily disappears after disruptions
- Strong collisional wave damping due to plasma cooling can justify the extinction of kinetic instabilities.
- However, such quiescent phases are often terminated by sequences of violent instabilities;
- this happens if the RE beam lasts long enough (> 0.2 s typical) under the action of position-controlled current ramp-down.

17. Anomalous Doppler resonances

Figure 9

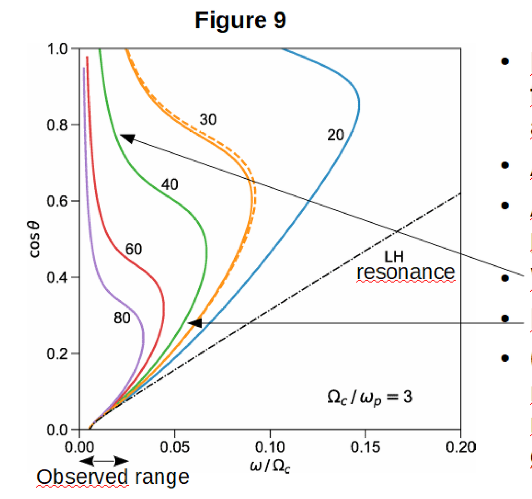

$$\omega = (k_\parallel c p_\parallel - \Omega_c)/\gamma$$

- Resonance curves in frequency – propagation angle diagram
- At different Lorentz factors
- At 0 (solid) or 0.1 (dashed) pitch angle.
- Whistler branches
- LH branches
- 0.003 – 0.025 range of measured frequencies normalized to electron gyrofrequency

- Resonance with whistler waves falls in the observed range only for γ > 30, i.e. energy > 15 MeV.

18. Conclusions and perspectives

- Radio emission by RE electrons was measured on FTU, both on low-density hot plasmas and on post-disruption RE beams.
- Explored conditions included ω_{ce}/ω_{pe} > 3, in the ballpark of ITER start-up values.
- Further FTU data analysis will be submitted for publication before the end of 2021.

Collaborations

- COMPASS: A collaboration with IPP-CAS (Prague) started in 2020. A large number of RE instabilities were measured and data are now under analysis.
- TCV: Preliminary test of RF detection by ex-vessel antennas performed in 2020. Measurements with in-vessel antenna, already agreed with the TCV team, should be carried out between the end of 2021 and the beginning of 2022.